

Optical excitation spectrum of an atom in a surface-induced potential

Fam Le Kien,^{1,*} S. Dutta Gupta,^{1,2} and K. Hakuta¹

¹*Department of Applied Physics and Chemistry, University of Electro-Communications, Chofu, Tokyo 182-8585, Japan*

²*School of Physics, University of Hyderabad, Hyderabad, India*

(Dated: October 3, 2018)

We study the optical excitation spectrum of an atom in the vicinity of a dielectric surface. We calculate the rates of the total scattering and the scattering into the evanescent modes. With a proper assessment of the limitations, we demonstrate the portability of the flat-surface results to an experimental situation with a nanofiber. The effect of the surface-induced potential on the excitation spectrum for free-to-bound transitions is shown to be weak. On the contrary, the effect for bound-to-bound transitions is significant leading to a large excitation linewidth, a substantial negative shift of the peak position, and a strong long tail on the negative side and a small short tail on the positive side of the field-atom frequency detuning.

PACS numbers: 42.50.Vk, 42.50.-p, 32.80.-t, 32.70.Jz

The study of individual neutral atoms in the vicinity of dielectric and metal surfaces has gained renewed interest due to progress in atom optics and nanotechnology [1, 2, 3, 4, 5, 6, 7]. The ability of manipulating atoms near surfaces has established them as a tool for cutting-edge applications such as quantum computation [8, 9, 10], atom chips [11, 12], and probes, very sensitive to the surface-induced perturbations [13]. Recently, translational levels of an atom in a surface-induced potential have been studied [1, 2, 3, 4]. An optical technique for loading atoms into quantum adsorption states of a dielectric surface has been suggested [1, 2]. An experimental observation of the excitation spectrum of cesium atoms in quantum adsorption states of a nanofiber surface has been reported [3]. Spontaneous radiative decay of translational levels of an atom near a dielectric surface has been investigated [4]. In this paper, we study the optical excitation spectrum of an atom in a surface-induced potential.

We assume the whole space to be divided into two regions, namely, the half-space $x < 0$, occupied by a nondispersive nonabsorbing dielectric medium (medium 1), and the half-space $x > 0$, occupied by vacuum (medium 2). We examine an atom, with an upper internal level e and a lower internal level g , moving in the empty half-space $x > 0$.

The potential energy of the surface-atom interaction is a combination of a long-range van der Waals attraction $-C_3/x^3$ and a short-range repulsion [14]. Here C_3 is the van der Waals coefficient. We approximate the short-range repulsion by an exponential function $Ae^{-\alpha x}$, where the parameters A and α determine the height and range, respectively, of the repulsion. The combined potential depends on the internal state of the atom (see Fig. 1), and is presented in the form $V_j(x) = A_j e^{-\alpha_j x} - C_{3j}/x^3$, where $j = e$ or g labels the internal state of the atom. The potential parameters C_{3j} , A_j , and α_j depend on the dielectric and the atom. In numerical calculations, we use the parameters of fused silica, for the dielectric, and the parameters of atomic cesium with the D_2 line, for the two-level atomic model. According to Ref. [4], the

parameters of the ground- and excited-state potentials for the silica-cesium interaction are $C_{3g} = 1.56 \text{ kHz } \mu\text{m}^3$, $C_{3e} = 3.09 \text{ kHz } \mu\text{m}^3$, $A_g = 1.6 \times 10^{18} \text{ Hz}$, $A_e = 3.17 \times 10^{18} \text{ Hz}$, and $\alpha_g = \alpha_e = 53 \text{ nm}^{-1}$.

We introduce the notation $\varphi_a \equiv \varphi_{\nu_e}$ and $\varphi_b \equiv \varphi_{\nu_g}$ for the eigenfunctions of the center-of-mass motion of the atom in the potentials V_e and V_g , respectively. They are determined by the stationary Schrödinger equations

$$\left[-\frac{\hbar^2}{2m} \frac{d^2}{dx^2} + V_j(x) \right] \varphi_{\nu_j}(x) = \mathcal{E}_{\nu_j} \varphi_{\nu_j}(x). \quad (1)$$

Here m is the mass of the atom. The eigenvalues $\mathcal{E}_a \equiv \mathcal{E}_{\nu_e}$ and $\mathcal{E}_b \equiv \mathcal{E}_{\nu_g}$ are the total center-of-mass energies of the translational levels of the excited and ground states, respectively. These eigenvalues are the shifts of the energies of the translational levels from the energies of the corresponding internal states. Without the loss of generality, we assume that the center-of-mass eigenfunctions φ_a and φ_b are real functions.

FIG. 1: Energies and wave functions of the center-of-mass motion of the ground- and excited-state atoms in the surface-induced potentials. The parameters of the potentials are $C_{3g} = 1.56 \text{ kHz } \mu\text{m}^3$, $C_{3e} = 3.09 \text{ kHz } \mu\text{m}^3$, $A_g = 1.6 \times 10^{18} \text{ Hz}$, $A_e = 3.17 \times 10^{18} \text{ Hz}$, and $\alpha_g = \alpha_e = 53 \text{ nm}^{-1}$. The mass of atomic cesium $m = 132.9 \text{ a.u.}$ is used. We plot, for the excited state, two bound levels ($\nu = 400$ and 415) and, for the ground state, two bound levels ($\nu = 281$ and 285) and one free level ($\mathcal{E}_f = 4.25 \text{ MHz}$).

We introduce the combined eigenstates $|a\rangle = |e\rangle \otimes |\varphi_a\rangle$ and $|b\rangle = |g\rangle \otimes |\varphi_b\rangle$, which are formed from the internal and translational eigenstates. The corresponding energies are $\hbar\omega_a = \hbar\omega_e + \mathcal{E}_a$ and $\hbar\omega_b = \hbar\omega_g + \mathcal{E}_b$. Here, ω_j with $j = e$ or g is the frequency of the internal level j . Then, the Hamiltonian of the atom moving in the surface-induced potential can be represented in the diagonal form $H_A = \sum_a \hbar\omega_a |a\rangle \langle a| + \sum_b \hbar\omega_b |b\rangle \langle b|$. We emphasize that the summations over a and b include both the discrete

($\mathcal{E}_{a,b} < 0$) and continuous ($\mathcal{E}_{a,b} > 0$) spectra. The levels a with $\mathcal{E}_a < 0$ and the levels b with $\mathcal{E}_b < 0$ are called the bound (or vibrational) levels of the excited and ground states, respectively. In such a state, the atom is bound to the surface. It is vibrating, or more exactly, moving back and forth between the walls formed by the van der Waals potential and the repulsion potential. The levels a with $\mathcal{E}_a > 0$ and the levels b with $\mathcal{E}_b > 0$ are called the free (or continuum) levels of the excited and ground states, respectively. The center-of-mass wave functions of the bound levels are normalized to unity. The center-of-mass wave functions of the free levels are normalized to the delta function of energy. For bound states, the center-of-mass wave functions φ_a and φ_b can be labeled by the quantum numbers ν_a and ν_b , respectively. For free levels, the conventional sums over a and b must be replaced by the integrals over \mathcal{E}_a and \mathcal{E}_b , respectively.

Suppose that the atom is driven by a coherent plane-wave laser field $\mathbf{E}_1 = [\mathcal{E}e^{-i(kx+\omega t)}\boldsymbol{\epsilon} + \text{c.c.}]/2$, propagating perpendicularly to the surface of the dielectric. Here \mathcal{E} , $\boldsymbol{\epsilon}$, ω , and $k = \omega/c$ are the envelope, the polarization vector, the frequency, and the wave number, respectively, of the laser field. The field reflected from the surface is $\mathbf{E}_2 = -R[\mathcal{E}e^{i(kx-\omega t)}\boldsymbol{\epsilon} + \text{c.c.}]/2$, where $R = (n_1 - 1)/(n_1 + 1)$ is the reflection coefficient. According to Ref. [4], the time evolution of the density matrix ρ of the atom is governed by the equations

$$\begin{aligned}\dot{\rho}_{aa'} &= \frac{i}{2} \sum_{l,b} (\Omega_{lab} \rho_{a'b}^* e^{-i\delta_{ab}t} - \Omega_{la'b}^* \rho_{ab} e^{i\delta_{a'b}t}) \\ &\quad - \frac{1}{2} (\gamma_a + \gamma_{a'}) \rho_{aa'}, \\ \dot{\rho}_{ab} &= \frac{i}{2} \sum_{l,b'} \Omega_{lab'} \rho_{b'b} e^{-i\delta_{ab'}t} - \frac{i}{2} \sum_{l,a'} \Omega_{la'b} \rho_{aa'} e^{-i\delta_{a'b}t} \\ &\quad - \frac{1}{2} \gamma_a \rho_{ab}, \\ \dot{\rho}_{bb'} &= -\frac{i}{2} \sum_{l,a} (\Omega_{lab'} \rho_{ab}^* e^{-i\delta_{ab'}t} - \Omega_{la'b}^* \rho_{ab'} e^{i\delta_{ab}t}) \\ &\quad + \frac{1}{2} \sum_{aa'} (\gamma_{aa'bb'} + \gamma_{a'ab'b}) e^{i(\omega_{bb'} - \omega_{aa'})t} \rho_{aa'},\end{aligned}\quad (2)$$

where the parameters $\gamma_{aa'bb'}$ and $\gamma_a \equiv \sum_b \gamma_{aabb}$ are the radiative decay coefficients [4], the index $l = 1$ or 2 labels the incident or reflected field, respectively, the notation $\delta_{ab} = \omega - \omega_a + \omega_b$ stands for the detuning of the field frequency ω from the atomic transition frequency $\omega_{ab} = \omega_a - \omega_b$, and the quantities

$$\begin{aligned}\Omega_{1ab} &= \Omega F_{ab}(-k) = \Omega F_{ab}^*(k), \\ \Omega_{2ab} &= -R \Omega F_{ab}(k)\end{aligned}\quad (3)$$

are the Rabi frequencies of the fields $\mathbf{E}_{l=1,2}$ with respect to the translational-state transition $a \leftrightarrow b$. Here, $\Omega = \mathcal{E}d_{eg}/\hbar$ is the Rabi frequency of the driving field with respect to the transition between the internal states $|e\rangle$ and $|g\rangle$, with $d_{eg} = \boldsymbol{\epsilon} \cdot \langle e|\mathbf{d}|g\rangle$ being the projection of

the atomic dipole moment onto the polarization vector $\boldsymbol{\epsilon}$. The coefficient

$$F_{ab}(k) = \langle \varphi_a | e^{ikx} | \varphi_b \rangle \quad (4)$$

is the overlapping matrix element that characterizes the transition between the center-of-mass states $|\varphi_a\rangle$ and $|\varphi_b\rangle$ with a transferred momentum of $\hbar k$. Since φ_a and φ_b are real functions, we have $F_{ab}(-k) = F_{ab}^*(k)$. In deriving Eqs. (3), we have neglected the cross decay coefficients $\gamma_{aa'} \equiv \sum_b \gamma_{aa'bb}$ with $a \neq a'$. Such coefficients are small compared to the radiative linewidths γ_a and $\gamma_{a'}$ when the refractive index n_1 of the dielectric is not large [4].

We plot in Fig. 2 the Frank–Condon factors $|F_{ab}(k)|^2$ for three bound ground-state levels ν_b and various bound excited-state levels ν_a . As seen from the figure, a deep bound ground-state level can be substantially coupled to a deep excited-state level. A deeper lower level can substantially overlap with a deeper upper level. The level $\nu_b = 285$, with translational energy shift $\mathcal{E}_b = -54.39$ MHz, can be substantially coupled to the level $\nu_a = 400$, with translational energy shift $\mathcal{E}_a = -132.84$ MHz. The difference $\mathcal{E}_a - \mathcal{E}_b = -78.45$ MHz is negative and large compared to the natural linewidth $\gamma_0 = 5.25$ MHz of the D_2 line of atomic cesium. In principle, both types of shifts, namely red (negative) shifts ($\mathcal{E}_a - \mathcal{E}_b < 0$) and blue (positive) shifts ($\mathcal{E}_a - \mathcal{E}_b > 0$), of the transition frequencies may be obtained. Note that the van der Waals potential for the excited state is stronger than that for the ground state. Therefore, for a bound-to-bound transition with a substantial Frank–Condon factor, the energy shift of the excited-state level is usually larger than that of the ground-state level. Consequently, the strong bound-to-bound transitions usually have red shifts. Since the depths of the surface-induced potentials V_g and V_e are large (159.6 THz for V_g and 316 THz for V_e), the range of the frequency shifts of the strong bound-to-bound transitions is broad, and the shifts can reach large negative values.

We plot in Fig. 3 the Frank–Condon factors $|F_{ab_f}(k)|^2$ for a free ground-state level b_f and various bound excited-state levels a . The figure shows that the values of the Frank–Condon factors $|F_{ab_f}(k)|^2$ are more substantial for shallow bound excited-state levels than for deep ones. Among the bound excited-state levels, the level that is most strongly coupled to the free ground-state level b_f is the level with the quantum number $\nu_a = 415$. The translational energy shift of this level is $\mathcal{E}_a = -6.56$ MHz. This bound level of the excited state is rather shallow. Due to this fact, the frequency shift $\mathcal{E}_a - \mathcal{E}_{b_f} = -10.81$ MHz of the strongest free-to-bound transition from the free level $\mathcal{E}_{b_f} = 4.25$ MHz is negative but not large. We note that, when the temperature of the atomic system is low, the typical values of the free-level energy \mathcal{E}_{b_f} are small. In this case, the range of the frequency shifts of substantial free-to-bound transitions is small compared to the range of the frequency shifts of substantial bound-to-bound transitions.

We now calculate the excitation spectrum of the atom

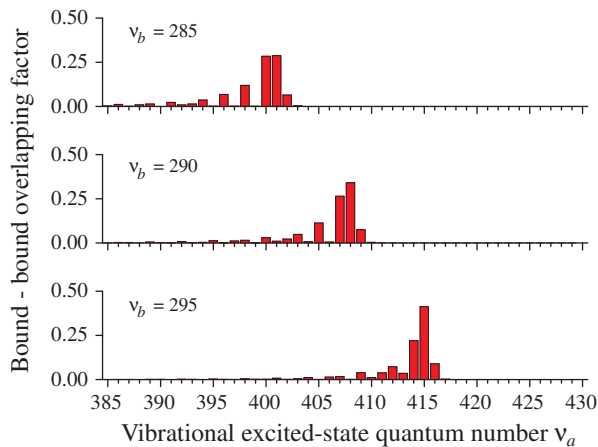


FIG. 2: Frank-Condon factors $|F_{ab}(k)|^2$ for three bound ground-state levels b , with $\nu_b = 285, 290$, and 295 , and various bound excited-state levels a , with ν_a in the range from 385 to 430. The light wavelength is $\lambda = 852$ nm. Other parameters are as in Fig. 1.

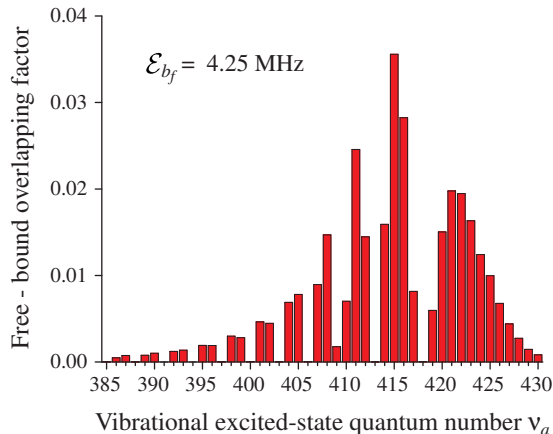


FIG. 3: Frank-Condon factors $|F_{ab_f}(k)|^2$ for a free ground-state level b_f , with $\mathcal{E}_{b_f} = 4.25$ MHz, and various bound excited-state levels a , with ν_a in the range from 385 to 430. The parameters used for calculations are as in Fig. 2.

in the surface-induced potential. Assume that the field is so weak that the Rabi frequency Ω is much smaller than the natural linewidth γ_0 . We also assume that the atom is initially in a coherent mixtures of the ground-state levels b with the weight factors $\rho_{bb} = \rho_{bb}(0)$, which are the initial populations of the levels. We consider the adiabatic regime. We find from Eqs. (2) that the population ρ_{aa} of the excited-state level a is given by

$$\rho_{aa} = \frac{s}{2} \sum_b \frac{\gamma_0^2}{\gamma_a^2 + 4\delta_{ab}^2} |F_{ab}^*(k) - RF_{ab}(k)|^2 \rho_{bb}, \quad (5)$$

where $s = 2|\Omega|^2/\gamma_0^2$ is the saturation parameter. The rate of total scattering of light from the atom is given by

$\Gamma_{sc} = \sum_a \rho_{aa} \gamma_a$. With the help of Eq. (5), we find

$$\Gamma_{sc} = \frac{s}{2} \sum_{ab} \frac{\gamma_0^2}{\gamma_a^2 + 4\delta_{ab}^2} \gamma_a |F_{ab}^*(k) - RF_{ab}(k)|^2 \rho_{bb}. \quad (6)$$

We note that, due to the presence of the interface, the field in a mode can be either a propagating light wave or a bound evanescent wave [15, 16]. An evanescent wave appears on the vacuum side of the interface when a light beam passing from the dielectric to the vacuum is totally internally reflected. Therefore, we can decompose the spontaneous emission rate as $\gamma_a = \gamma_a^{(ev)} + \gamma_a^{(rad)}$, where $\gamma_a^{(ev)}$ and $\gamma_a^{(rad)}$ are the rates of spontaneous emission from the level a into the bound evanescent modes and the propagating radiation modes, respectively [4]. Hence, we have $\Gamma_{sc} = \Gamma_{sc}^{(ev)} + \Gamma_{sc}^{(rad)}$, where

$$\Gamma_{sc}^{(ev)} = \frac{s}{2} \sum_{ab} \frac{\gamma_0^2}{\gamma_a^2 + 4\delta_{ab}^2} \gamma_a^{(ev)} |F_{ab}^*(k) - RF_{ab}(k)|^2 \rho_{bb}. \quad (7)$$

is the rate of scattering from the atom into the evanescent modes and $\Gamma_{sc}^{(rad)} = \Gamma_{sc} - \Gamma_{sc}^{(ev)}$ is the rate of scattering from the atom into the propagating radiation modes.

All the above results were derived for a two-level atom moving in a potential induced by an infinite flat surface, and Eqs. (6) and (7) represent the rigorous expressions for the rates of the total scattering and the scattering into the evanescent modes (in the framework of the adiabatic approximation and the perturbation theory). However, with a proper assessment of the limitations, the above theory can be applied to typical experimental situations. As an example, we pick a recent experiment [3], whereby, the number of photons scattered from cesium atoms into the guided modes of a nanofiber was measured as a function of the frequency of the probe field. To apply our flat-surface results to the situation of a nanofiber, we use several assumptions and approximations. First of all, we note that, in the case of an atom near a fiber, the effective potential for the center-of-mass motion of the atom along the radial direction must include the centrifugal potential $U_{cf} = \hbar^2(l_z^2 - 1/4)/2mr^2$. Here l_z is the quantum number for the axial component of the angular momentum of the atom. Since the van der Waals potential is $U_{vdW} = C_3/r^3$, we have $|U_{cf}| \ll |U_{vdW}|$ when the condition $r \ll r_c \equiv 2mC_3/(\hbar^2|l_z^2 - 1/4|)$ is satisfied. Thus, when the atom is near to the fiber surface and the axial angular momentum is small, the effect of the centrifugal is small compared to that of the van der Waals potential. In this case, we can neglect the centrifugal potential. For cesium atoms with $m = 132.9$ a.u. and $l_z = 10$, the condition for the validity of the above approximation is $r \ll r_c \cong 411$ nm. Next, we note that the reflection of an incident plane wave from a cylindrical surface is rather complicated; it does not produce a plane wave. However, for the silica-vacuum interface, the reflection coefficient for light with wavelength $\lambda = 852$ nm is $R \cong 0.18$, a small number. Therefore, to simplify our calculations,

we can neglect the reflection of light from the fiber surface. Finally, we note that there are two types of modes of the field in the presence of a nanofiber, namely guided modes and radiation modes. The guided modes are characterized by evanescent waves on the outside of the fiber. They are then the direct analog of the evanescent modes of a dielectric–vacuum interface.

For a cesium atom at rest, the rate $\gamma(r)$ of total spontaneous emission and the rate $\gamma^{(g)}(r)$ of spontaneous emission into the guided modes of a nanofiber have been calculated systematically in Ref. [6]. For an atom in a translational state $|a\rangle$, the rate γ_a of total spontaneous emission and the rate $\gamma_a^{(g)}$ of spontaneous emission into the guided modes can be estimated as [4]

$$\begin{aligned}\gamma_a &= \int_0^\infty \gamma(r) |\varphi_a(r)|^2 dr, \\ \gamma_a^{(g)} &= \int_0^\infty \gamma^{(g)}(r) |\varphi_a(r)|^2 dr.\end{aligned}\quad (8)$$

We plot in Fig. 4 the rates γ_a and $\gamma_a^{(g)}$ for a nanofiber with radius of 200 nm, which was used in the experiment [3]. Figure 4 shows that the emission into the guided modes is substantial for a wide range of bound excited-state levels ($\nu_a < 430$). However, when ν_a is very large ($\nu_a \geq 430$), the channeling of emission into the guided modes becomes negligible. The reason is that, when ν_a is very large the bound state is very shallow. The atom in such state spends most of its time far away from the surface, where the evanescent waves in the guided modes cannot penetrate into.

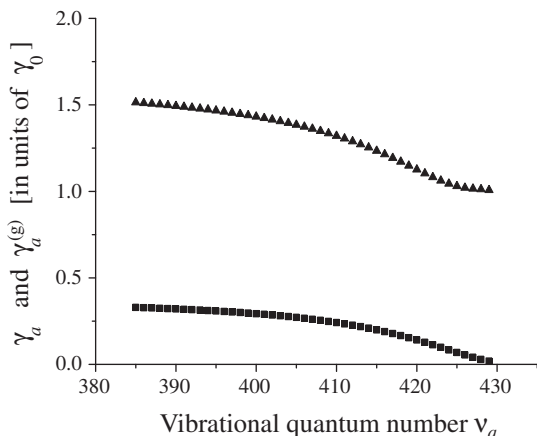


FIG. 4: Rate of total spontaneous emission, γ_a (triangles), and rate of spontaneous emission into the guided modes, $\gamma_a^{(g)}$ (squares), for a nanofiber. The parameters for the surface–atom potentials are as in Fig. 1. The atomic transition wavelength is $\lambda_0 = 852$ nm. The fiber radius is 200 nm. All the rates are averaged with respect to the orientation of the dipole moment.

With the above simplifications and approximations, the rate of scattering into the guided modes of a nanofiber

can be estimated by

$$\Gamma_{sc}^{(g)} = \frac{s}{2} \sum_{ab} \frac{\gamma_0^2}{\gamma_a^2 + 4\delta_{ab}^2} \gamma_a^{(g)} |F_{ab}(k)|^2 \rho_{bb}. \quad (9)$$

The dependence of $\Gamma_{sc}^{(g)}$ on the field–atom detuning $\delta = \omega - \omega_0$ (the difference between the probe field frequency ω and the free-space atomic resonance frequency ω_0) characterizes the optical excitation spectrum of the atom in the surface-induced potential. We calculate $\Gamma_{sc}^{(g)}$ for two cases. In the first case, the atom is initially in free ground-state levels. In the second case, the atom is initially in bound ground-state levels. We plot the results for the first and second cases in Figs. 5 and 6, respectively.

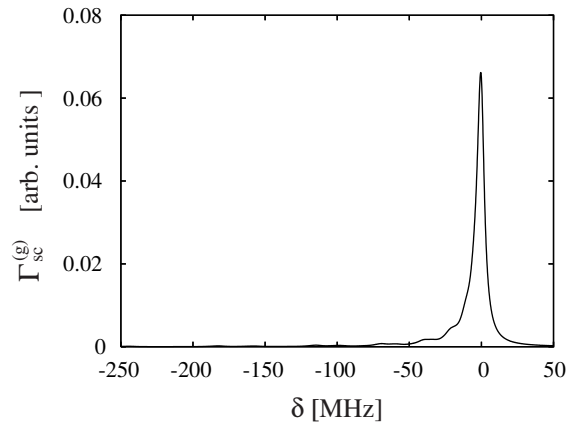


FIG. 5: Rate $\Gamma_{sc}^{(g)}$ of light scattering from the atom into the guided modes of a nanofiber through the free-to-bound transitions as a function of the detuning $\delta = \omega - \omega_0$ of the probe field. The atom is initially in a thermal mixture of free ground states with temperature $T = 200$ μ K. The range of the quantum numbers ν_a of the bound excited states involved into the calculations is from 385 to 429. The natural linewidth of the atom is $\gamma_0 = 5.25$ MHz. Other parameters are as in Figs. 1 and 4.

In the first case, i.e. the case of Fig. 5, we assume that the initial state of the atom is a thermal mixture of free ground states $|b_f\rangle$, described by the density operator

$$\rho(0) = |g\rangle\langle g| \int_0^\infty P_E |E\rangle\langle E| dE. \quad (10)$$

Here, $|E\rangle$ are the continuum eigenstates, normalized to the delta function of energy, for the ground-state Hamiltonian $p^2/2m + V_g(r)$, and $P_E = e^{-E/k_B T}/Z$ is the Boltzmann weight factor, with T and Z being the temperature and partition function, respectively, for the atomic system. The dependence of the scattering rate $\Gamma_{sc}^{(g)}$ on the field detuning δ in Fig. 5 represents the optical excitation spectrum for the atomic free-to-bound transitions. This spectrum shows a small negative shift of about -0.4 MHz for the position of the peak. The linewidth of the spectrum is about 6.7 MHz, slightly larger than the natural

linewidth $\gamma_0 = 5.25$ MHz of the D_2 line of atomic cesium. In addition, the spectrum has a small, short tail on the negative side of the detuning. These features are the results of the negative frequency shifts of the transitions between free ground-state levels and bound excited-state levels. The observed effects are however weak, and the excitation spectrum is basically concentrated around the atomic resonance frequency ω_0 . The reason is the following: The Frank–Condon factor for the overlap between a free ground-state and a deep bound excited-state level is small (see Fig. 3). Therefore, a free ground-state atom can be excited only to shallow bound levels (and free levels) of the excited state. Meanwhile, an atom in a shallow (or free) excited level cannot emit photons efficiently into the guided modes because the atom spends most of its time far away from the fiber (see Fig. 4). Hence, the effect of the surface-induced potential on the excitation spectrum in the case of free-to-bound transitions is rather weak.

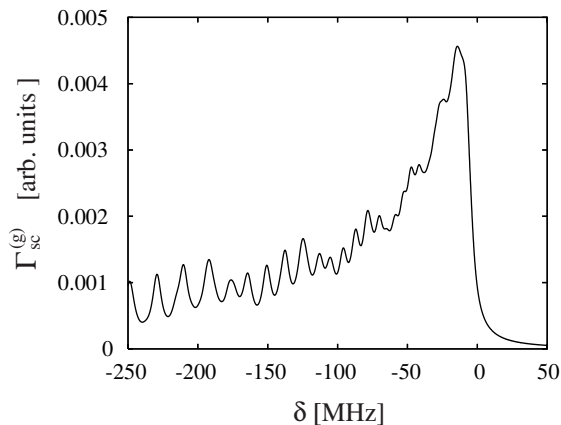


FIG. 6: Rate $\Gamma_{\text{sc}}^{(g)}$ of light scattering from the atom into the guided modes of a nanofiber through the bound-to-bound transitions as a function of the detuning $\delta = \omega - \omega_0$ of the probe field. The atom is initially in an incoherent mixture of a number of bound ground-state levels with quantum numbers ν_b from 269 to 293 and equal weight factors. The bound excited-state levels involved into the calculations are those with the quantum numbers ν_a from 385 to 429. The natural linewidth of the atom is $\gamma_0 = 5.25$ MHz. Other parameters are as in Figs. 1 and 4.

In the second case, i.e. the case of Fig. 6, we assume that the initial state of the atom is in an incoherent mixture of a number of bound ground-state levels ν_b , with flat weight factors $\rho_{bb} = \text{const}$. The initial density operator of the atom is given by

$$\rho(0) = \frac{1}{N} \sum_{\nu_b=\nu_{\min}}^{\nu_{\max}} |b\rangle\langle b|, \quad (11)$$

where N is the number of bound ground-state levels involved in the initial state of the atom. The use of flat weight factors is explained by the assumption that the

atom is adsorbed by a surface at the room temperature $T = 300$ K $\cong 6.25$ THz, which is much higher than the energy differences between the levels. For our numerical calculations, we include the bound ground-state levels with quantum numbers ν_b from 269 to 293. The energy shifts of these levels, equal to their total center-of-mass energies, are in the range from -1 GHz to -5 MHz. We do not include levels with larger quantum numbers because they are too shallow and therefore, an atom in such a bound ground-state level can be easily excited to a free ground-state level by heating or collision. We also do not include levels with smaller quantum numbers because the corresponding transition frequency shifts are beyond the range of the excitation spectrum measured in the experiment [3]. The dependence of the scattering rate $\Gamma_{\text{sc}}^{(g)}$ on the field detuning δ in Fig. 6 represents the optical excitation spectrum for the atomic bound-to-bound transitions. This spectrum shows a substantial negative shift of about -14.3 MHz for the position of the peak. The linewidth of the spectrum is about 58.3 MHz, which is one order larger than the natural linewidth $\gamma_0 = 5.25$ MHz of the D_2 line of atomic cesium. Furthermore, the spectrum has a substantial long tail on the negative side and a small short tail on the positive side of the detuning. These features are the results of the frequency shifts of the transitions between bound ground-state levels and bound excited-state levels. In general, both negative and positive shifts can come into play. However, the transitions with positive shifts are relatively weak because the corresponding Frank–Condon factors are usually small. The overlap between the center-of-mass wave functions of a bound excited-state level and a bound ground-state level is substantial only when the corresponding returning points are close to each other. Since the van der Waals potential for the excited state $|e\rangle$ is deeper than that for the ground state $|g\rangle$, the frequency shifts of the transitions that are associated with substantial Frank–Condon factors are mostly negative. The deeper the bound ground-state levels involved in the initial state, the stronger the effect of the surface–atom interaction on the excitation spectrum. We note that the basic features of the spectrum in Fig. 6 are very similar to the features of the right and left wings of the experimental spectrum reported in Ref. [3]. However, it is important to recall that the experimental spectrum [3] has contributions from both bound-to-bound and free-to-bound types of transitions. A combination of both Figs. 5 and 6 with proper weight factors can indeed lead to an excellent matching of the experimental spectrum with the theoretically predicted one.

In conclusion, we have studied the optical excitation spectrum of an atom in the vicinity of a dielectric surface. We have derived rigorous expressions for the rates of the total scattering and the scattering into the evanescent modes. With a proper assessment of the limitations, our theoretical results have been applied to an experimental situation with a nanofiber. We have shown that the effect of the surface-induced potential on the excitation spec-

trum in the case of free-to-bound transitions is rather weak. Meanwhile, the spectrum of excitation of bound-to-bound transitions has a large linewidth, a substantial negative shift of the peak position, and a substantial long tail on the negative side and a small short tail on the positive side of the field–atom frequency detuning. The basic features of the calculated spectra are in agreement with the experimental observations [3].

Acknowledgments

We thank M. Oriá, K. Nayak, and P. N. Melentiev for fruitful discussions. This work was carried out under the 21st Century COE program on “Coherent Optical Science.”

-
- [*] Also at Institute of Physics and Electronics, Vietnamese Academy of Science and Technology, Hanoi, Vietnam.
 - [1] E. G. Lima, M. Chevrollier, O. Di Lorenzo, P. C. Segundo, and M. Oriá, *Phys. Rev. A* **62**, 013410 (2000).
 - [2] T. Passerat de Silans, B. Farias, M. Oriá, and M. Chevrollier, *Appl. Phys. B* **82**, 367 (2006).
 - [3] K. P. Nayak *et al.* (submitted to *Phys. Rev. Lett.*).
 - [4] Fam Le Kien and K. Hakuta *et al.* (submitted to *Phys. Rev. A*).
 - [5] V. I. Balykin, K. Hakuta, Fam Le Kien, J. Q. Liang, and M. Morinaga, *Phys. Rev. A* **70**, 011401(R) (2004); Fam Le Kien, V. I. Balykin, and K. Hakuta, *Phys. Rev. A* **70**, 063403 (2004).
 - [6] Fam Le Kien, S. Dutta Gupta, V. I. Balykin, and K. Hakuta, *Phys. Rev. A* **72**, 032509 (2005).
 - [7] Fam Le Kien, V. I. Balykin, and K. Hakuta, *Phys. Rev. A* **73**, 013819 (2006).
 - [8] N. Schlosser, G. Reymond, I. Protsenko, and P. Grangier, *Nature (London)* **411**, 1024 (2001).
 - [9] S. Kuhr, W. Alt, D. Schrader, M. Müller, V. Gomer, and D. Meschede, *Science* **293**, 278 (2001).
 - [10] C. A. Sackett, D. Kielpinski, B. E. King, C. Langer, V. Meyer, C. J. Myatt, M. Rowe, Q. A. Turchette, W. M. Itano, D. J. Wineland, and C. Monroe, *Nature (London)* **404**, 256 (2000).
 - [11] R. Folman, P. Kruger, J. Schmiedmayer, J. Denschlag, and C. Henkel, *Adv. At. Mol. Opt. Phys.* **48**, 263 (2002).
 - [12] S. Eriksson, M. Trupke, H. F. Powell, D. Sahagun, C. D. J. Sinclair, E. A. Curtis, B. E. Sauer, E. A. Hinds, Z. Muktadir, C. O. Gollasch, and M. Kraft, *Eur. Phys. J. D* **35**, 135 (2005).
 - [13] J. M. McGuirk, D. M. Harber, J. M. Obrecht, and E. A. Cornell, *Phys. Rev. A* **69**, 062905 (2004).
 - [14] H. Hoinkes, *Rev. Mod. Phys.* **52**, 933 (1980).
 - [15] O. Di Stefano, S. Savasta, and R. Girlanda, *Phys. Rev. A* **61**, 023803 (2000).
 - [16] M. Born and E. Wolf, *Principles of Optics* (Pergamon, New York, 1980).

This figure "fig1.gif" is available in "gif" format from:

<http://arxiv.org/ps/quant-ph/0610067v1>